International Journal of GEOMATE, June, 2022, Vol.22, Issue 94, pp.1-12
ISSN: 2186-2982 (P), 2186-2990 (O), Japan, DOI: https://doi.org/10.21660/2022.94.j2392
Geotechnique, Construction Materials and Environment

SOURCE EXTRACTION OF ROCKFALL BY MICROTOPOGRAPHY HIGHLIGHT MAP VIA HIGH-DENSITY AERIAL LASER SURVEY

*Koki Sakita[1], Teruyuki Kikuchi[2] and Satoshi Nishiyama[1]

[1]Graduate School of Environmental and Life Science, Okayama University, Japan; [2] JP Design Co. Ltd., Tokyo, Japan

*Corresponding Author, Received: 11 Nov. 2021, Revised: 27 Jan. 2022, Accepted: 02 April 2022

ABSTRACT: Investigations using maps that reflect slope conditions have been conducted for slope inspection. However, oversight at the time of inspection has become a problem owing to unsatisfactory map performance. This paper presents a microtopography highlight map created using a high-density aerial laser survey as a new inspection tool and evaluates the influence of survey conditions on a desk study of rockfall sources using the map to develop an efficient slope inspection method. The microtomography highlight map is created by the combination of a slope map, which displays the slope angles, and a wavelet analysis map, which displays the unevenness of the slope. The slope and wavelet analysis maps are created via terrain analysis based on the digital elevation model, which is created using aerial laser survey results. In this study, we demonstrated slope inspection using a map of grid size 50 cm on two slopes where there was a risk of falling rocks. A comparison of the desk study and field research showed that using the map was effective in extracting the source of the rockfall (>2 m height). In addition, the verification results showed that the measurement conditions affect the representation of the map, and that the measurement should be conducted in winter to produce a more detailed map, which leads to effective inspection.

Keywords: Aerial laser survey, Terrain analysis, Slope inspection, Rockfall

1. INTRODUCTION

Owing to the increasing recent occurrence of heavy rain and earthquakes, the necessity to tackle disaster prevention planning on slopes is increasing. A rockfall is a slope disaster in which separated rock blocks are activated by a force and fall on a slope under the influence of gravity. Predicting the time and location of an occurrence of rockfall is extremely difficult. However, most rockfalls are caused by the destabilization and activity of the rocky part. Therefore, inspections are conducted while focusing on the rockfall source, to implement rockfall countermeasures (Fig.1). The slope inspection consists of a desk survey to select the inspection location using maps and a field survey to observe the selected location and understand the conditions. In conventional inspection methods, aerial photographs and contour lines, which are relatively easy to produce, have been used as inspection maps in desk surveys. However, in the current slope inspection method, accurately determining the position of the source of falling rock is difficult owing to the expression or positioning accuracy issues of inspection maps, and oversights have been reported in slope inspections [1].

Thus, the use of aerial laser surveying and terrain analysis technology has been considered to overcome this problem. Aerial laser surveying is being considered for use in various fields [2,3,4]. In addition, the use of aerial laser surveying for the extraction of rockfall sources has been studied. However, the representation of microtopography, particularly ridges and valleys, has been insufficient [5,6,7].

This study examines the usefulness of a microtopography highlight map using a high-density aerial laser survey in a desk study of rockfall sources. In addition, we focused on the measurement conditions of the aerial laser survey, such as the timing and direction of the measurement, and studied the influence of the aerial laser survey on the slope inspection.

Fig.1 Field survey photo showing an example of a source of rockfall

2. AERIAL LASER SURVEY AND DATA PROCESSING

2.1 Aerial Laser Survey

An aerial laser survey is a type of three-dimensional surveying technique that uses sensors mounted on aircraft [8]. The measurement is performed using a non-prism-type laser rangefinder mounted on an aircraft. The irradiated laser pulse strikes the ground surface and is reflected, and the distance is measured by acquiring the returned return pulse. For the survey, the aircraft is further equipped with a global navigation satellite system (GNSS) sensor and an inertial measurement unit (IMU) that measures the position and altitude of the aircraft during flight. The location information is corrected using the acquired sensor information to generate the 3D data comprising points. These data are called a point cloud. This surveying system can measure the topography of a slope, even in mountainous terrain with trees, as the laser reaches the ground surface. Therefore, this system is effective for understanding topographical changes in mountainous areas, which is difficult to achieve with the conventional method.

2.2 Data Processing of Point Cloud

In aerial laser surveying, three types of data exist in the processing process (Fig.2). The original data need to be handled first. These data are the as-measured data, which include data related to not only the ground surface but also the vegetation and noise on the slope. These unnecessary data are removed by the filtering process, and thus, ground data are created after the removal. However, the ground data may contain missing data depending on the measurement conditions. Therefore, the ground data were interpolated and supplemented to obtain uniform data. These uniform data are the grid data.

2.3 Terrain Analysis

Aerial laser data can be used for terrain analysis to calculate the amount of terrain that quantifies the unevenness and slope of the terrain from the 3D coordinates of the grid data [9,10]. In addition, a topographic analysis map is created by assigning colors according to the topography. The microtopography highlight map proposed in this study consists of three topographic analyses, and the method of creating this map is presented here. Such mapping technology using topographical analysis is expected to be used in the field of slope disaster prevention [11].

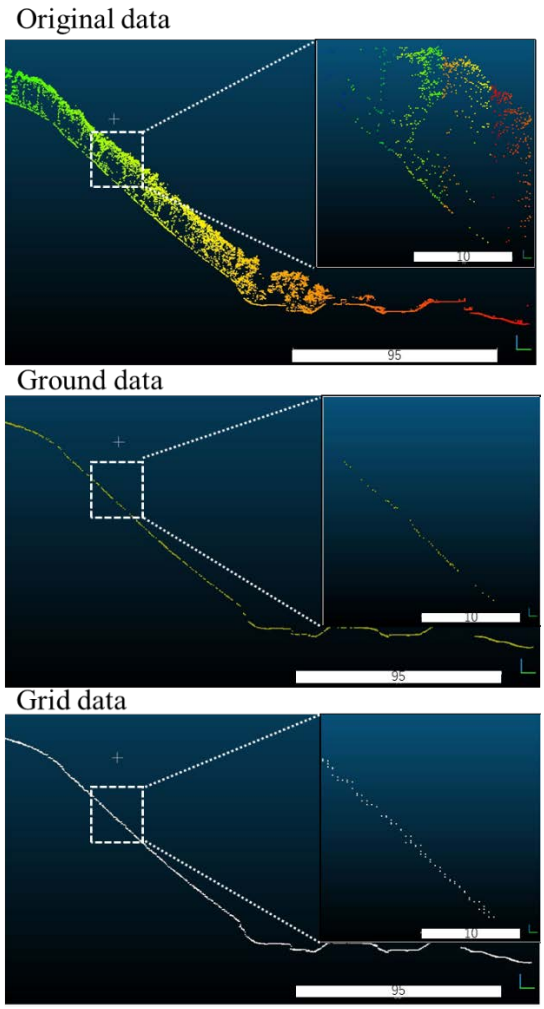

Fig.2 Example of aerial laser survey data processing process and data cross-section

2.3.1 Contour map

Contour maps are basic numerical maps. They are created by drawing a line connecting points of the same elevation on a map. The slope can be determined based on the coarseness and denseness of the contour lines, but the topographical changes between contour lines cannot be expressed.

2.3.2 Slope map

A slope map is a drawing in which the inclination amount for each pixel of the grid data is calculated, and the brightness is changed according to this value to represent the topography [12]. In this analysis, the inclination amount is calculated based on the elevation of the center point in a 3×3 manufacturing grid, as shown in Fig.3. Gentle slopes are represented with high brightness, and steep slopes are represented with low brightness; hence, the map has an appearance of three-dimensionality. However, as there is no information to show the difference in elevation, distinguishing between ridges and valleys is difficult when the terrain is small and complicated.

2.3.3 Wavelet analysis map

The wavelet analysis map expresses the undulation of the terrain by color according to the wavelet analysis. Here, Eq. (1) is a two-dimensional wavelet analysis [13].

$$C(s,a,b) = \frac{1}{s}\int_{-\infty}^{\infty}\int_{-\infty}^{\infty} z(x,y)\psi\left(\frac{x-a}{s},\frac{y-b}{s}\right)dx\,dy \quad (1)$$

The wavelet analysis map can be obtained by performing a convolution integral on a function ψ called a mother wavelet and a coordinate value z of a slope with arbitrary coordinates (a, b) and a shift amount s. In this study, the mother wavelet adopts the second derivative of the Gaussian function and takes a shape similar to the Mexican hat function (2).

$$\psi(x,y) = (2 - x^2 - y^2)\exp\left\{-\frac{1}{2}(x^2+y^2)\right\} \quad (2)$$

As there is no information indicating the height difference and slope, discerning the microtopography is difficult. A graph of the Mexican hat function drawn on a 3D mesh is shown in Fig.4.

2.3.4 Microtopography highlight map and transmission composition

The topographic analysis maps described above have various advantages in representation, but also have drawing-specific disadvantages. The disadvantages of these maps are evident when they are viewed as a standalone map; however, they can be used in conjunction with other maps to interpolate information. With the improved performance of personal computers, multiple topographic analysis drawings can be transparently combined. In this section, a microtopographic highlight map is created by combining the three drawings introduced above: a contour map, slope map, and wavelet analysis map.

The first step is to synthesize the slope quantity map using the slope information and the wavelet analysis map, which can easily distinguish the ridges and valleys. Thus, the two types of drawings compensate for their mutual shortcomings while maintaining their original characteristics. Furthermore, the slope undulations can be expressed by superimposing contour lines. Examples of these drawings are presented in Fig. 5. In the proposed method, we attempted to create a map suitable for expressing a mountainous area using a greenish color tone for the wavelet analysis map.

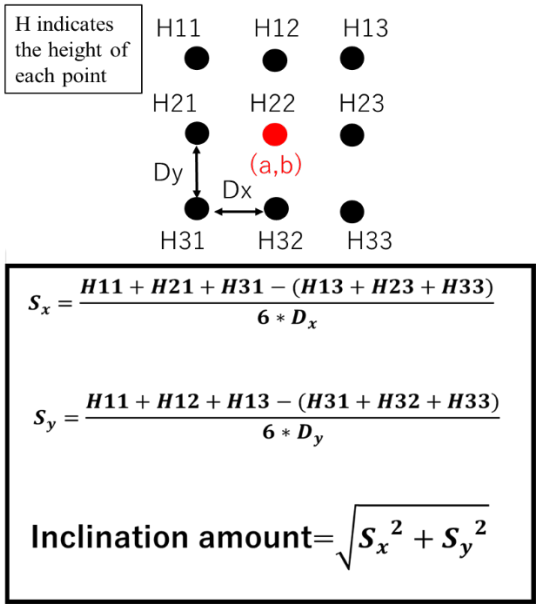

Fig.3 Analysis overview of the slope map

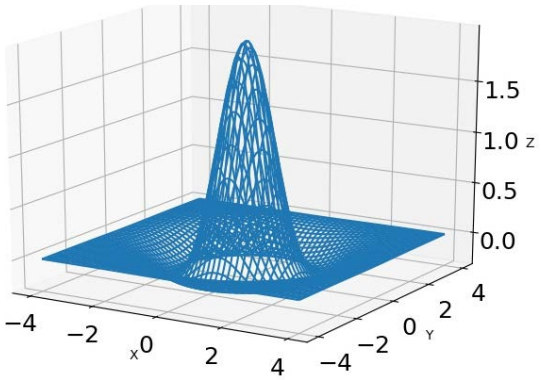

Fig.4 Mexican hat function

3. VERIFICATION OF DESK STUDY USING MICROTOPOGRAPHY HIGHLIGHT MAP

3.1 Survey and Measurement Overview

Based on the measurements performed on actual slopes, rockfall sources were inspected using microtopography highlight maps for verification. In particular, we verified the effect of different measurement conditions on the maps and extraction performance. Here, the timing of the aerial laser surveying and the measurement direction (longitudinal only or grid) were identified. In the Japanese environment, vegetation flourishes in mountainous areas in summer and in deciduous areas in winter. This difference in environmental conditions affects whether the laser reaches the ground surface during aerial laser surveying. In addition, the difference in the measurement direction affected the point density on the ground surface. Therefore, the relationship between the

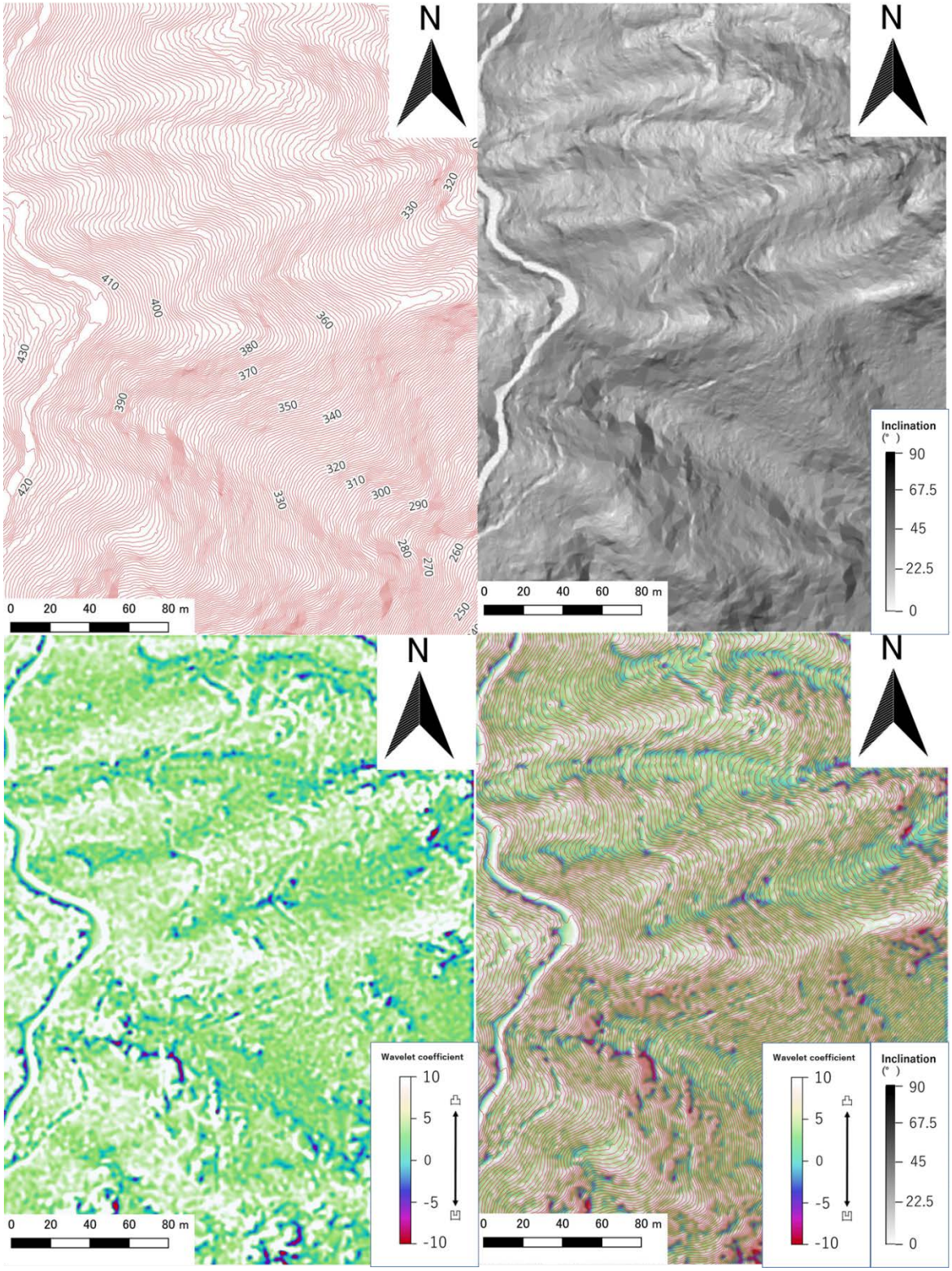

Fig.5 Topographic analysis maps created from the aerial laser survey data; top left: contour map (1 m pitch), top right: slope map, bottom left: wavelet analysis map, bottom right: microtopography highlight map

measurement conditions and the extraction performance was evaluated. This measurement was performed using the aerial laser surveying system shown in Fig.6.

The measurement data were used to create grid data according to the data processing flow, and the grid size was standardized to 50 cm. Then, contour maps, slope maps, and wavelet analysis maps were created. These maps were then superimposed to create a microtopography highlight map. The first

step in the survey was to conduct a desktop study of rockfall sources using a map. The areas identified in the desk study were visited in the field to confirm the existence of rockfall sources and their shapes. During the field survey, the extracted locations needed to be determined accurately. Therefore, the maps were imported into a tablet with a GNSS function, and a field survey was conducted while checking the self-position of the tablet and the symmetry of the maps [14].

3.2 Study Area

In this verification, the area around Tai, Takakura-cho, Takahashi City, Okayama Prefecture, Japan, on General Route 180 was selected. This route is designated as an emergency transportation road connecting Takahashi City and Niimi City and follows the Takahashi River and steep terrain. A photograph of the site is shown in Fig.7. As shown in the figure, vegetation thrives in the summer season, making it difficult to identify the location of the source of the fallen rocks from aerial photographs alone. Geological analysis showed that the site was composed of andesite of the Late Mesozoic Cretaceous Period. Rocks have been reported to have fallen in the past, and some have reached the road.

3.3 Differences in the Extraction of Rockfall Sources using Microtopography Highlight Maps from Two Different Periods

In this section, the influence of the results of measurements performed at two different times on the maps is examined. Accordingly, the differences in the measurement results between the two periods were first examined. Table 1 shows the point densities calculated from the measurement data for the two periods. The measurements were performed at both periods so that the planning point density was 14 points per square meter. However, there was a difference in the number of irradiations between the two periods. The number of irradiations was higher in the measurements during summer. Nevertheless, the point density was higher in winter for both the original and

LiteMapper6800-400		
Operating AGL		30-1600 m
Scan angle		45 – 60 °
Pulse rate		80,000 – 400,000 Hz
Number of scans		10 - 200 Hz
Beam diameter		0.5 mrad
Laser safety standard		Class3R
Nominal ocular hazard area		>1.5m(NOHD), >10m(ENOHD)
Measurable altitude	Pulse rate	Maximum operating AGL
	80,000 Hz	1600 m
	200,000 Hz	1100 m
	300,000Hz	950 m
	400,000 Hz	800 m
Equipment		GNSS/IMU : IGI AEROcontrol-II Digital camera:DigiCAM-50

Fig.6 Aerial laser survey and survey specification table used for measurements

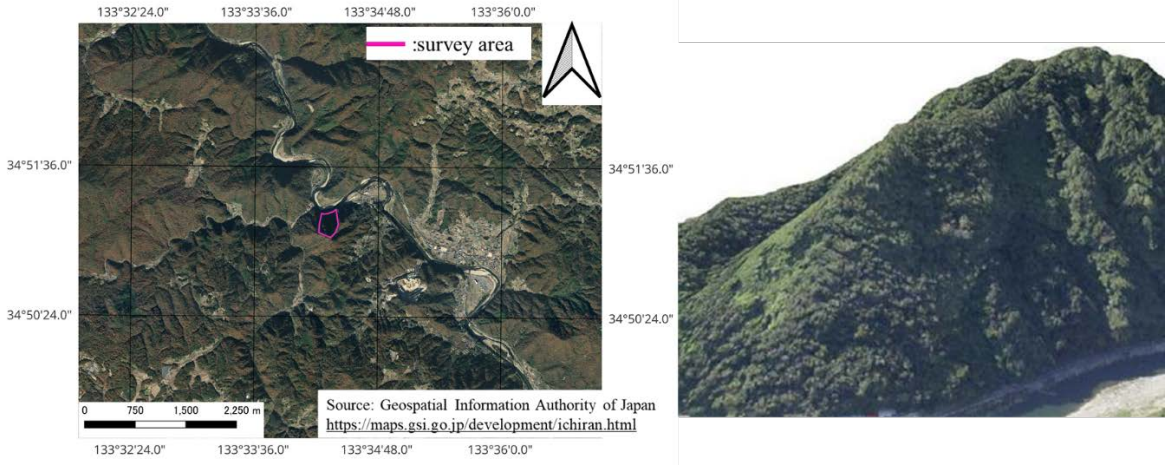

Fig.7 Photos of the experimental site: Tai, Takakura-cho, Takahashi City, Okayama Prefecture, Japan. Left: aerial photo (created by processing Geographical Survey Institute tiles); right: field photo.

Table 1 Point cloud data results for each measurement period

Measurement Data	Season	Planning point density	Number of irradiations	Original data point density	Ground data point density
October, 2014	Summer	14	4,454,825	51.496	1.840
December, 2015	Winter	14	3,912,460	82.755	6.859

ground data. In aerial laser surveying, the number of data points increases according to the number of reflections. Therefore, when measured in winter, the laser beam could easily reach under the tree canopies due to the effect of falling leaves, and the number of reflections from branches, leaves, and ground surface increased, leading to an increase in the number of data points.

Subsequently, the desk-based extraction of rockfall source locations was performed with microtopography enhancement maps based on the data from the two periods. The wavelet analysis map shows positive values (white in the legend) for the rockfall sources on the microtopography map because the topography is convex, whereas the slope map shows high values (black in the legend) for the cliffs. A desk survey was conducted using these values as a reference. A field survey was conducted to confirm the consistency of the results of the desk study. The results of these comparisons are presented in Fig. 8. In this figure, the rockfall sources that could be extracted in both maps are indicated by orange circles. For example, Nos. 1–3 in Fig.8 correspond to this category. On the other hand, some areas could be extracted only with winter data, which are represented by green circles. These areas are Nos. 4, 5, and 9 (for example). Finally, the areas that could not be extracted from the data of both seasons are represented by blue circles. These areas are Nos. 7 and 11 (for example).

No. 8 in the figure shows a rockfall source with a height of 8.0 m, which could be extracted in both maps. In addition, the rockfall source No. 26, which has a height of 3.0 m, was successfully identified in both maps. In contrast, the rockfall sources Nos. 39 and 49, which have a specific height of 6.0 m, could be extracted only with the winter data. This was the case for almost half of the locations surveyed in this study.

In addition, several rockfall sources could not be extracted in both maps. Among them, rockfall source No. 14 could not be extracted in both maps even though its specific height was 3.0 m. The results of the field survey showed that the laser could not reach the ground surface because of the lack of leaf fall in both winter and summer. In addition, the boulders shown in No. 17, which were already separated and scattered in the middle of the slope, could not be extracted by this method because the size of the rock mass was smaller than that of the source of the fallen rocks.

3.4 Differences in the Extraction of Rockfall Sources using Microtopography Highlight Maps from Two Different Measurement Directions

Subsequently, the effect of different measurement directions on the extraction performance was examined. Here, two types of measurements were performed: one with 50% wrapped measurements in the longitudinal direction only, and the other with 50% wrapped measurements in a grid. These measurements were conducted in winter with reference to the results in the previous section, and the point densities and map of the grid measurements are the same as the results in Table 1 and Fig.8, respectively.

The point density of the ground data was calculated from the measured data in the longitudinal direction only, and it was 3.4 points per square meter. As shown in the results in Table 1, the point density of the ground data in the grid measurement is approximately 7 points per square meter, which is approximately twice the result of the longitudinal measurement only.

Subsequently, the microtopography highlight maps prepared under these two conditions, and the maps organizing the results of the desk and field surveys are shown in Fig.9. In this figure, the extracted rockfall sources for the two measurement conditions are shown in different colors. Thus, it was confirmed that most of the extracted rockfall sources were extracted from the data measured under both conditions. Therefore, only four rockfall sources could be extracted by grid measurement only. The locations that could not be extracted by both measurement conditions were the same as those shown in Fig.8.

3.5 Evaluation of the Effect of Different Measurement Conditions on the Extraction of Rockfall Sources

Tables 2 and 3 show the number of extractions for each category classified based on the size of the microtopography based on the extraction results shown in Figs.8 and 9 and the information on microtopography obtained from the field survey. As shown in Table 2, all the categories of rockfall sources showed a higher number of extractions in the winter data results. In particular, among the 14 rockfall sources with a specific height of 2.0 m to 3.0 m, 13 were

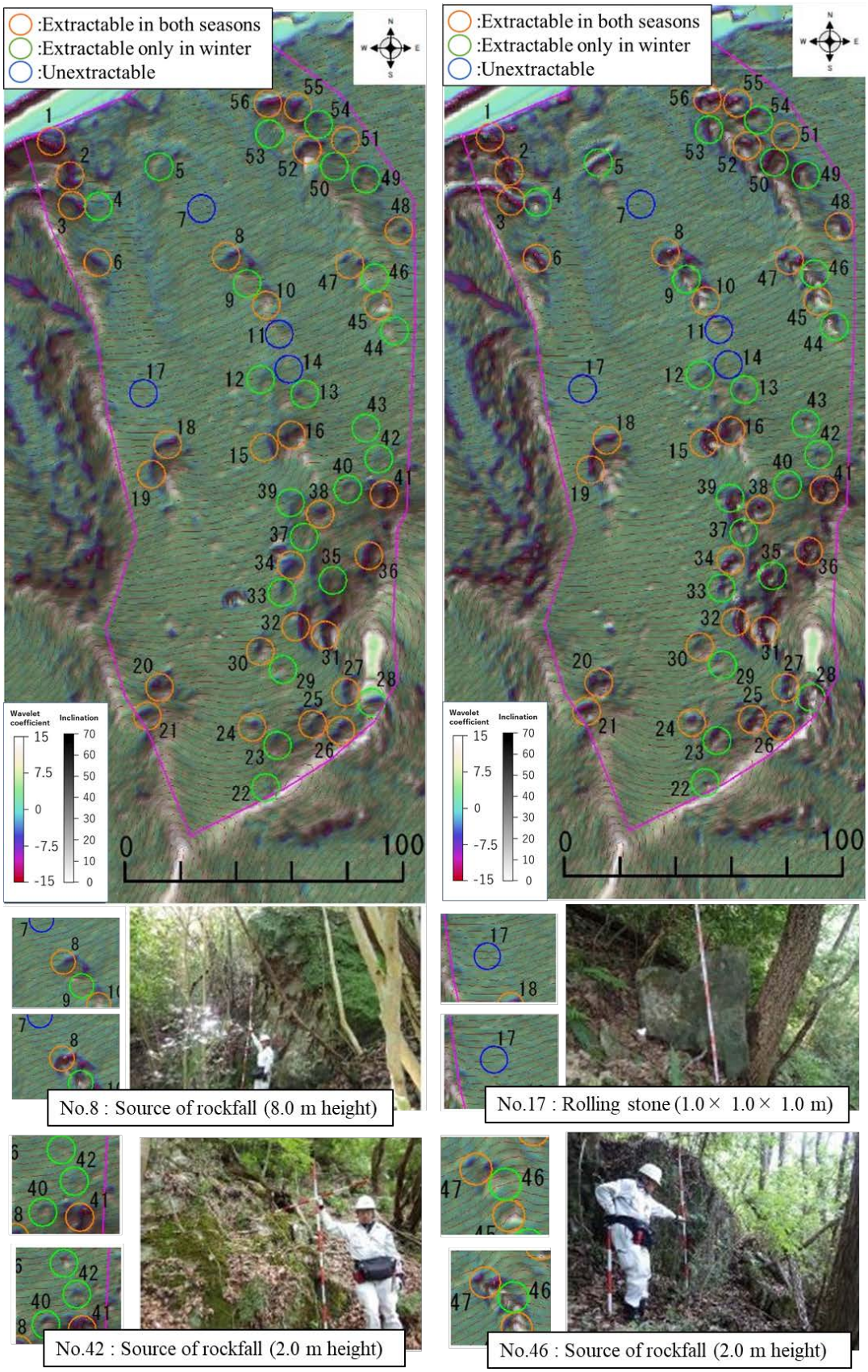

Fig.8 Two microtopography highlight maps created from the measurement data of two periods (left: summer data, right: winter data). The circles on the map are the extraction results classified based on the results of desk and field surveys. The lower part of the image shows the field survey image and a magnified view of the corresponding area.

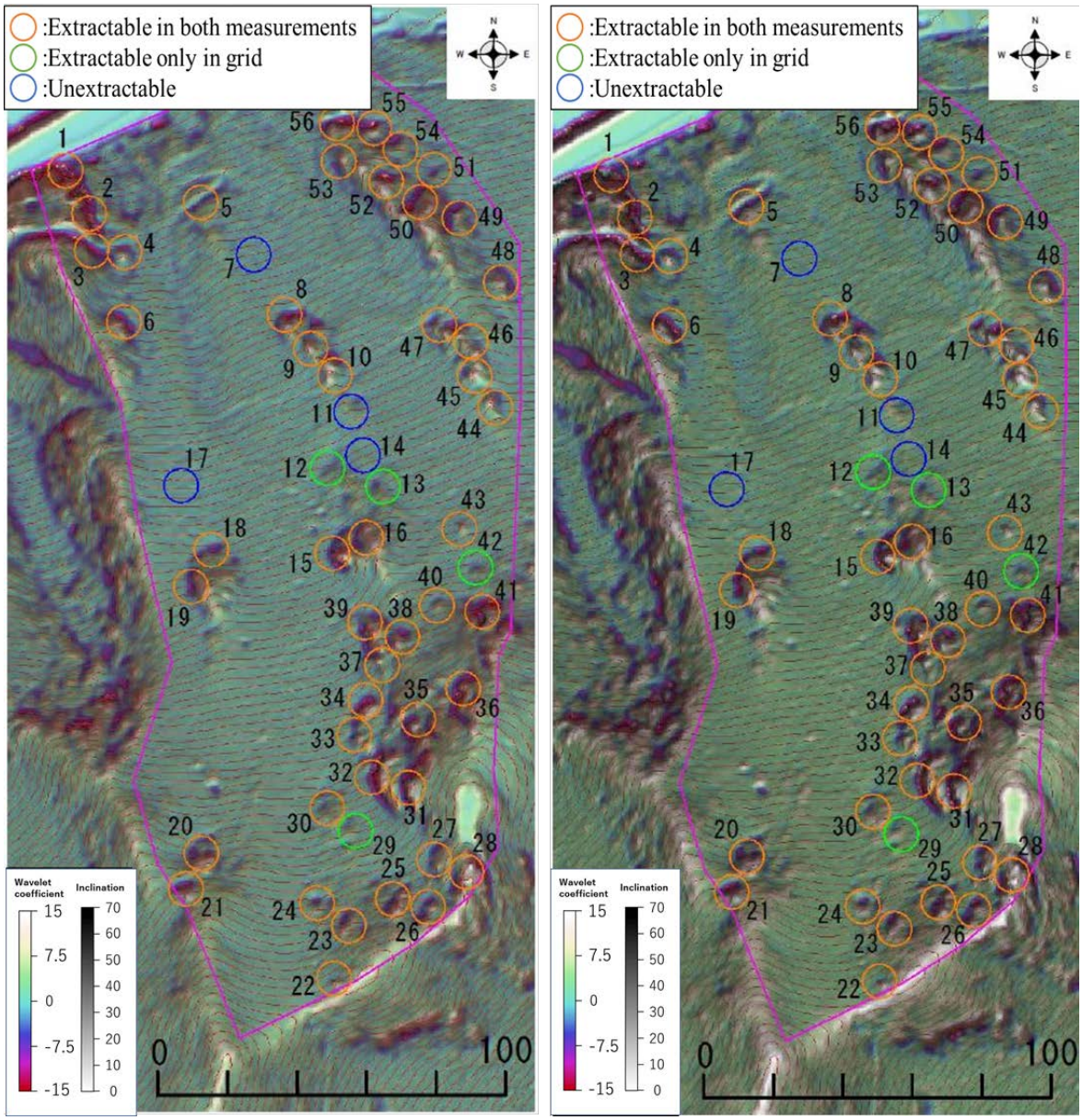

Fig.9 Two microtopography highlight maps produced from the two measurement directions (left: longitudinal measurement only, right: grid measurement). The circles on the map are the extraction results classified based on the results of desk and field surveys.

identified by the desk survey from the winter data, whereas only two were identified from the summer data. Table 3 shows the differences in the number of extractions owing to the differences between the two measurement directions by category. In the longitudinal measurement, only nine rockfall sources with a specific height of 2.0 m to 3.0 m were extracted. However, only one extraction was not possible for those sources with a specific height over 3.0 m, which is the same as the desktop extraction result using the map of the grid measurement. As mentioned earlier, the boulders at the two locations could not be extracted under all the conditions in the present results, and these results were confirmed to be useful only for the source of falling rocks.

In this measurement, there were differences in the ground data owing to the differences in the measurement period and measurement direction. In addition, the number of extracted rockfall sources in the microtopography map created from these data was different. In particular, the difference in the timing of measurement had a significant impact on the extraction performance. In Table 2, the number of rockfall sources with a relatively small specific height of 2.0 m to 3.0 m was larger than that of rockfall sources with a large specific height of more than 4.0 m. This suggests that the difference in measurement timing affects the number of rockfall sources with such a small specific height. On the other hand, for different measurement directions, there was a difference in

the point density of the ground data, but there was no significant difference in the number of extracted rockfall sources. If the measurement direction is changed from longitudinal to grid measurement, the cost will be higher because the length of the measurement will be longer. Therefore, if the results of the longitudinal measurement alone are equivalent to those of the grid measurement, the longitudinal measurement should be considered during the period of leaf fall.

4. VERIFICATION OF FALLING ROCK SOURCE EXTRACTION BY MICROTOPOGRAPHY USING LONGITUDINAL MEASUREMENT DATA OF ROADS IN WINTER AT OTHER SITES

Based on the results of the previous chapter, the validity of the suggested measurement conditions needs to be examined. In this section, the extraction performance of the rockfall source is verified at other sites.

The site used for verification was a slope along the Fukumoto–Wake Route in Mimasaka City, Okayama Prefecture (Fig.10). Several rockfall sources have been confirmed at this site. Geological analysis of this site shows that it is composed of alternating layers of sandstone and mudstone from the Early Triassic Period of the Mesozoic Era. Measurements were performed in February 2017 under defoliated conditions. The ground data were generated from the measured data and analyzed. The point density of the ground data was 4 points per square meter. The microtopographic highlight and the results of the survey at the study site are shown in Fig.11.

Table 2 Number of extracted topographies classified by categories for the microtopography highlight maps created based on the measurement results of the two periods. The number in parentheses under each category is the number of inspection points in the field survey.

	Categories of extracted microtopography			
	2.0 m–3.0 m (14)	3.0 m–4.0 m (11)	>4.0 m (29)	Rolling stone (2)
Summer measurement	2	5	22	0
Winter measurement	13	10	29	0

Table 3 Number of extracted topographies classified by categories for the microtopography highlight maps created based on the two types of measurement directions. The number in parentheses under each category is the number of inspection points in the field survey.

	Categories of extracted microtopography			
	2.0 m–3.0 m (14)	3.0 m–4.0 m (11)	>4.0 m (29)	Rolling stone (2)
Longitudinal measurement only	9	10	29	0
Grid measurement	13	10	29	0

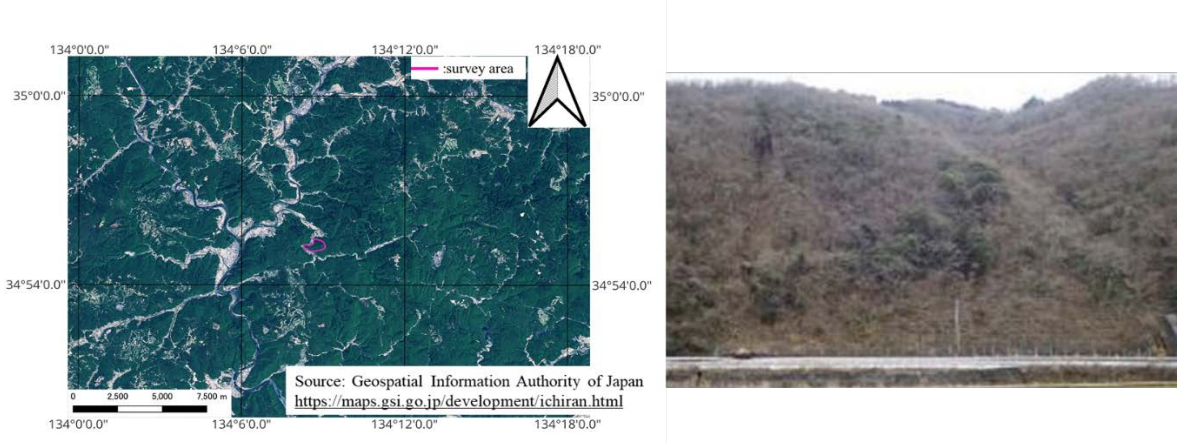

Fig.10 Photos of the experimental site: Fukumoto–Wake Route in Mimasaka City, Okayama Prefecture, Japan. left: aerial photo (created by processing Geographical Survey Institute tiles), right: field photo

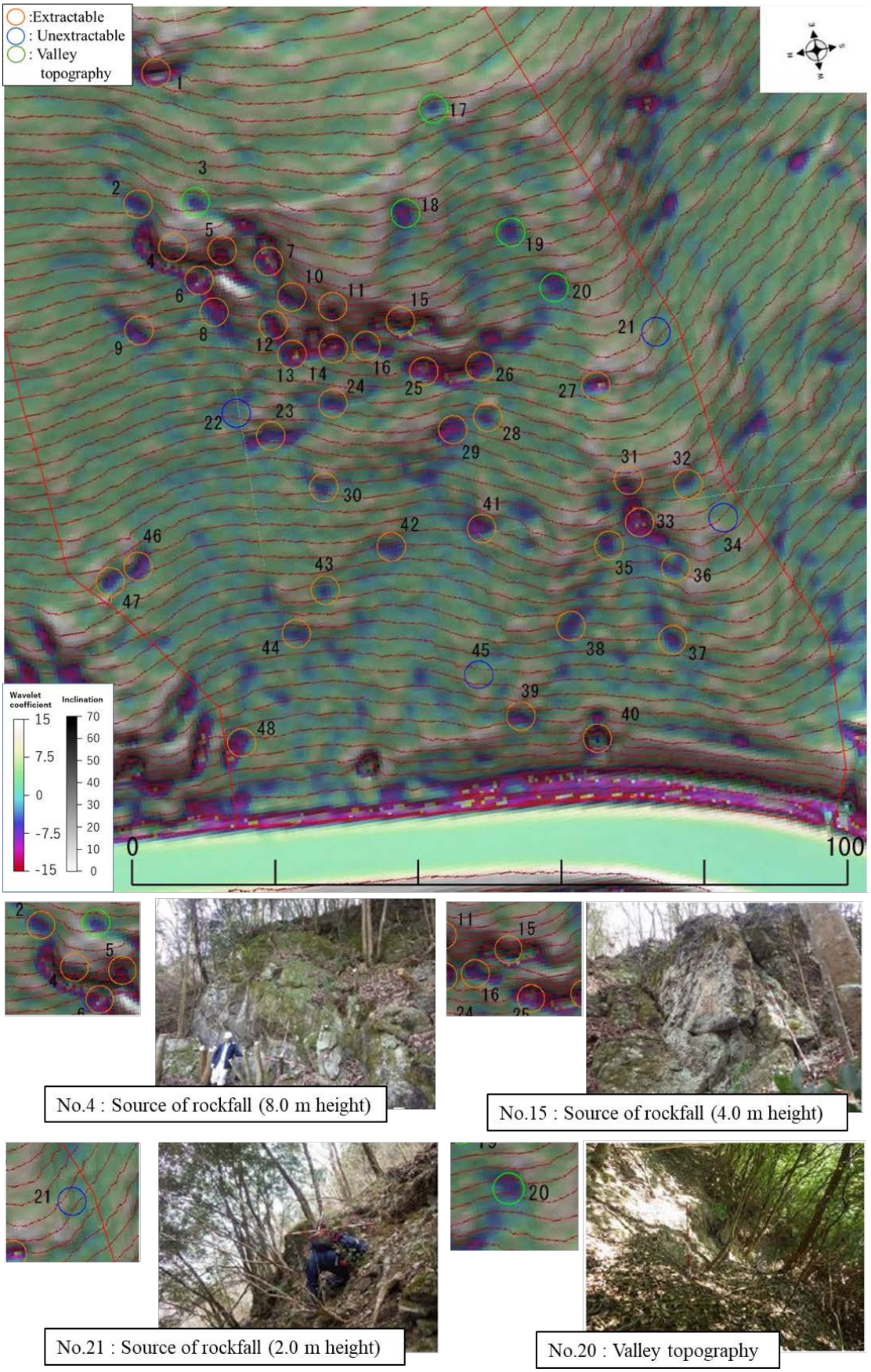

Fig.11 Microtopography highlight map created based on longitudinal measurement data in winter. The lower part of the image shows the field survey image and a magnified view of the corresponding area.

A field survey confirmed the existence of 48 topographic features at this site. Of these, the features that can be extracted on the map by desk survey are indicated by orange circles, and those that cannot be extracted are indicated by blue circles. Consequently, we extracted more than half of the rockfall sources from the desktop survey using the map at this site. However, four features could not be extracted. Three of these features were rolling stones, and the remaining was a rockfall source with a height of 2.0 m (No. 21). In addition to the rockfall sources, collapsed terrain in the form of valleys could be extracted through the desk survey. These valleys are indicated by green circles, and a total of five locations were identified. In addition, the upper and lateral sides of the microtopography exhibited a white color on the microtopography highlight map. This is different from the characteristics of the rockfall source shown earlier, suggesting that such differences can be used to distinguish the topography.

5. CONCLUSION

In this study, we proposed a method for extracting rockfall sources by using a microtopography highlight map created using high-density laser data and verified its extraction accuracy. It was confirmed that this map is useful for the representation of rockfall sources distributed over a wide area. Therefore, the use of microtopography maps in desktop investigations of rockfall sources can be a useful tool for improving inspection accuracy. In this study, we examined the effects of different measurement conditions on drawings and surveys. The results suggest that the timing of measurement affects the efficiency of the survey, and that conducting the aerial laser survey during the defoliation period maximizes the inspection effectiveness.

The proposed desktop survey with a microtopography highlight map can be a useful tool for extracting rockfall sources and other microtopographies. However, this method is limited to the extraction of the drawing, and the degree of danger of each microtopography on the drawing cannot be determined. Therefore, a field survey of the extracted areas needs to be conducted to confirm the shape and stability of the microtopography through the eyes of an expert.

The technology of aerial laser surveying has been progressing in recent years, and drone-mounted measurement systems have recently been developed [15]. The drone laser surveying system can measure at a lower altitude than the airborne system used in this study, which dramatically increases the number of laser points that can capture the ground surface [16]. Therefore, more detailed and precise data can be obtained. However, the drone itself has a limited flight time owing to battery problems, and its measurement range is narrower than that of an aircraft system. Therefore, the characteristics of each of these systems need to be determined, and the use of these systems in a suitable manner needs to be studied. In recent years, the use of artificial intelligence technology for slope disaster prevention has also been considered [17,18,19]. Deciphering has so far relied heavily on the experience and knowledge of experts, and the results have varied depending on the person performing the task. Therefore, this process needs to be unified so that the same results can be obtained by anyone. In the future, we plan to construct a slope disaster prevention system that incorporates these cutting-edge technologies.

6. REFERENCES

[1] Sasaki Y. and Asai K., Effectiveness of Disaster Prevention Inspections and Reduction of Disasters - Transitions and Challenges of Disaster Prevention Measures over the Past 10 Years. [translated from Japanese], https://www.zenchiren.or.jp/geocenter/lec-.

[2] Kikuchi T., Hatano T., Senda Y., and Nishiyama S., Development of Analytic Method for Landslide Measurement by Movement Vectors Using S-DEM Data Obtained from Airborne Laser Point Clouds, Journal of the Japan Society of Engineering Geology, Vol. 57, Issue 6, 2017, pp. 277-288.

[3] Monnet J. M., Clouet N., Bourrier F., and Berger F., Using geomatics and airborne laser scanning for rock fall risk zoning: a case study in the French Alps, The 2010 Canadian Geomatics Conference and ISPRS Commission I Symposium, Calgary, AB, Canada, 2010.

[4] Wilson M. F. J., O'Connell B., Brown C., Guinan J. C., and Grehan A. J., Multiscale terrain analysis of multibeam bathymetry data for habitat mapping on the continental slope, Marine Geodesy, Vol. 30, 2007, pp. 3-35.

[5] Tonini, M. and Abellan, A., Rockfall detection from terrestrial LiDAR point clouds: A clustering approach using R, Journal of Spatial Information Science, Vol. 8, 2014, pp. 95-110.

[6] Loye A., Jaboyedoff M., and Pedrazzini A., Identification of potential rockfall source areas at a regional scale using a DEM-based geomorphometric analysis, Natural Hazards and Earth System Sciences, Vol. 9, Issue 5, 2009, pp. 1643-1653.

[7] Losasso L., Jaboyedoff M., and Sdao F., Potential rock fall source areas identification and rock fall propagation in the province of Potenza territory using an empirically distributed approach, Landslides, Vol. 14, Issue 5, 2017, pp. 1593-1602.

[8] Wehr A. and Lohr U., Airborne laser scanning—an introduction and overview, ISPRS Journal of Photogrammetry and Remote Sensing, Vol. 54, Issue 2-3, 1999, pp. 68-82.
[9] Yokoyama R., Sirasawa M., and Kikuchi Y., Representation of topographical features by opennesses, Journal of the Japan Society of Photogrammetry and Remote Sensing, Vol. 38, Issue 4, 1999, pp. 26-34.
[10] Ishii H., Nishii R., and Takeda T., Guide for creating and interpreting maps for landslide topography interpretation using aerial laser survey data [draft] [translated from Japanese], Technical memorandum of PWRI, 2016, p. 4344.
[11] Guzzetti F., Mondini A. C., Cardinali M., Fiorucci F., Santangelo M., and Chang K. T., Landslide inventory maps: New tools for an old problem, Earth-Science Reviews, Vol. 112, 2012, pp. 42-66.
[12] Kamiya I., Tanaka K., Hasegawa H., Kuroki T., Hayata Y., Odagiri S., and Masaharu H., Production of slope map and its application, Geoinformatics, Vol. 10, Issue 2, 1999, pp. 76-79.
[13] Booth A. M., Roering J. J., and Prron J. T., Automated landslide mapping using spectral analysis and high-resolution topographic data: Puget Sound Lowlands, Washington, and Portland Hills, Oregon, Geomorphology, Vol. 109, 2009, pp. 132-147.
[14] Yoshikawa K., Miyashita M., Hamada N., Sakita K., and Nishiyama S., Method for efficient falling rock investigation using tablet type GIS and microtopography highlight map, Journal of Japan Society of Civil Engineers, Ser. F3, Vol. 74, Issue 2, 2018, pp. 121-131.
[15] Ngadiman N., Badrulhissaham A. I., Mohamad M., Azhari N., Kaamin M., and Hamid B. N., Monitoring Slope Condition Using UAV Technology, Civil Engineering and Architecture, Vol. 7, Issue 6A, 2019, pp. 1-6.
[16] Kikuchi T., Sakita K., Hatano T., and Nishiyama S., Topographic interpretation and quantification of landslide terrain deformation using aerial laser measurement data, Geoinformatics, Vol. 31, Issue 2, 2020, pp. 37-45.
[17] Ghorbanzadeh O., Meena R. S., Blaschke T., and Aryal J., UAV-Based Slope Failure Detection Using Deep-Learning Convolutional Neural Networks, Remote Sensing, Vol. 11, Issue 17, 2016, pp. 2046.
[18] Sakita K., Kikuchi T., Nishiyama S., Song J., and Ohnishi Y., Automatic extraction of rockfall source based on terrain analysis map using support vector machine, IOP Conference Series: Earth and Environmental Science, 861, 2021.
[19] Fanos A. M., Pradhan B., Mansor S., Yusoff Z. M., Abdullah A. Fb., and Jung H., Rockfall source identification using a hybrid Gaussian mixture-ensemble machine learning model and LiDAR data, Korean Journal of Remote Sensing, Vol. 35, Issue 1, 2019, pp. 93-115.

Copyright © Int. J. of GEOMATE All rights reserved, including making copies unless permission is obtained from the copyright proprietors.